Date of Publication: 14th May 2026
ISSN: 2737-713X

GROUND SHAKING IN ACCRA: UNVEILING SITE EFFECTS THROUGH AMBIENT NOISE

*Christian Owusu-Appiah, Thomas Enyimah Kaku Armah and Elikplim Abla Dzikunoo
Department of Earth Science, University of Ghana
***Corresponding author:** chrisoappiah23@gmail.com

Abstract
Local site conditions can significantly influence earthquake ground motion, increasing potential damage to buildings and infrastructure. The soils in the Greater Accra Metropolitan Area (GAMA) have complex lithologies with varying distributions, primarily due to the influence of bedrock, drainage, and topography. The history of damaging earthquakes, combined with the rapid expansion of urban development in the region, has further increased the exposure to seismic risk. The study aims to assess site effects and seismic vulnerability in this region using the horizontal-to-vertical spectral ratio (HVSR) analysis on passive ambient noise from 13 sites. The analysis reviewed key parameters including the fundamental site frequency (0.73 – 11.02 Hz), amplification factor (1.66 – 9.94), alluvium thickness (2.61 – 175.75 m), and soil vulnerability index (0.37 – 20.00). Tesano PS was identified as the most vulnerable site to earthquake destruction and liquefaction, reflecting its softer and thicker alluvial soils. In contrast, Lapaz exhibited a comparatively low seismic response, consistent with stiffer rocks with no amplification. Aburi, on the other hand, exhibited a low seismic response consistent with its shallower soils and more competent, rocky subsoil. These findings highlight the need to integrate site-specific parameters as determined above into land-use planning and the design of earthquake-resistant infrastructure in Accra.

Keywords
Earthquake, Site effects, HVSR, Ambient noise, Fundamental frequency, Amplification factor, Vulnerability index, Greater Accra Metropolitan Area

Introduction

Background

Earthquakes are among the most destructive natural disasters that have troubled civilizations from ancient times. They can reshape entire landscapes, cause significant loss of life, and damage a country's economic development. In recent decades, rapid urbanization and population growth globally, have concentrated people and infrastructure in cities which may be built on sedimentary basins (Fäh et al., 1997). Such areas may have been previously avoided due to geotechnical risks. These soft sediment layers act as amplifiers, intensifying ground motion and damage during earthquakes. The earthquake intensity and damage do not solely depend on the magnitude and distance from the epicentre. They also depend to a great extent on the soil characteristics, the underlying geological conditions, and engineering structural integrity (Akkaya and Özvan, 2019; Cadet et al., 2011; Janusz et al., 2022; Mundepi et al., 2015; Tanjung et al., 2021). The soil's structure plays a significant role in increasing the region's earthquake risk as well as the severity of the earthquake damage. Adjacent regions subjected to the same seismic activity may experience damage of varying scale including ones at a distance or remote from the epicentre, due to changes in geological conditions as the waves travel (Akkaya and Özvan, 2019; Bonnefoy-Claudet et al., 2009; Talha Qadri et al., 2015). In 2001, Ahmedabad (India) was severely affected by the Bhuj earthquake, even though the city was 400 km away from the epicentre. This earthquake had a magnitude of 7.7 on the Richter scale. This occurrence is due to the geology and younger alluvial deposits (Ranjan, 2005). Interestingly, soils that show stability under static stress may behave differently under dynamic stresses such as earthquakes, causing failure and massive destruction to structures (Akkaya and Özvan, 2019). Thick soft sediments with less compaction generally amplify the earthquake waves the most (Bard, 1994; Bonnefoy-Claudet et al., 2006; Tanjung et al., 2021). Comparatively, hard rock conditions cause the area experiencing an earthquake to record less damage (Damayanti and Sismanto, 2021). Vella et al. (2013) concluded that the thick layers of Oligocene-Miocene clay and marl greatly influence the site response of the Maltese islands and have a strong link with some of the most damaging earthquakes recorded in the area. Gurler et al. (2000) emphasised the relation between the geology of Mexico and the damage recorded and observed during the 1957 (magnitude 7.8) and 1985 (magnitude 8.0) earthquakes in the country. Most of the damaged buildings were situated on soft clays, which amplified the ground motion. Site effects refer to the variations in ground motion and seismic intensity felt at various regions as a result of the site's geology and geotechnical characteristics. Site effects significantly impact the severity of earthquake damage. Notable examples of site effects include the Great Hanshin-Awaji earthquake in Kobe in 1995, where a magnitude of 6.9 with an intensity ranging between XI to XII on the Modified Mercalli Intensity Scale was observed (Bonnefoy-Claudet et al., 2009).

Site effects estimation has emerged as a key tool to be used in developing mitigation strategies and possibly preventing structural damage resulting from seismic ground motion (Cadet et al., 2011). Such estimations are critical because different sites exhibit particular seismic responses at which ground motion is amplified and has proved to be disastrous when it coincides with the fundamental frequencies of buildings and

structures (Talha Qadri et al., 2015). Active fault zones and ground deformations also increase the risk of seismic hazards damaging infrastructure (Bray, 2009; Meghraoui et al., 2016; Murbach et al., 1999; Oettle and Bray, 2013). Bray (2009) highlighted that the performance of structures is greatly affected by site-specific factors such as fault characteristics, underlying surface geology, and the foundation of the structural system. Anastasopoulos et al. (2007) explained how the Atatürk Basketball Court in Turkey having its foundation overlying a displacement fault, was significantly damaged beyond repair. However, Murbach et al. (1999) showed that proper planning achieved less damage to some structures during the M 7.3 1992 Landers Earthquake event. In recent times, planning and management of urban areas has generally been based on economic considerations rather than geotechnical. These omissions during urban centre planning may result in greater damage than necessary with far-reaching economic and social implications in the event of a natural disaster (Chen et al., 2021; Janusz et al., 2022; Moustafa et al., 2022).

For earthquakes, magnitude, timing, and location cannot be predicted precisely. Hence, countries in both high and low-seismically hazardous areas have invested in pre-disaster mitigation strategies like building codes that inform design criteria for new construction works and also reinforce old buildings, as well as public awareness programmes. These strategies show how prepared the areas are and in effect, can reduce damage to properties and loss of lives. These strategies involve estimating the seismic vulnerability of a particular area by evaluating site effect parameters such as the fundamental frequency and the amplification factor to aid in geotechnical planning of new structures and also guide reinforcement or enhancement of old buildings (Bard, 1994; Bonnefoy-Claudet et al., 2006). Seismic vulnerability maps have been developed through geotechnical investigations to assist engineers in determining where various structures can be sited based on the building codes.

Over the years, various categories of methods have sought to estimate the magnitude of amplification caused by soft sediments. Amplification of ground motion is a result of the impedance contrast existing between the bedrock and soft sediments deposited on them (Castellaro and Mulargia, 2009; Hunter et al., 2002; Nortey et al., 2018). Numerous instances of catastrophic earthquake effects recorded in literature have shown the need to incorporate reliable analytical methods and procedures in site effect estimations (Marcellini, 2006). Methods that involve direct monitoring of ground motion through earthquakes are most effective and are limited to regions with high seismic activity rates. Such methods are less effective and rarely used in low to moderate seismic zones, as it takes several years to collect enough reliable datasets. Recent site effect assessments in urban and densely populated areas are based on ambient noise (Bonnefoy-Claudet et al., 2006; Janusz et al., 2022; Johnson and Lane, 2016; Liu et al., 2014). Ambient noise is a low-amplitude and short-period vibration sourced from natural disturbances such as wind interacting with structures and vegetation or from cars, heavy machinery, traffic, and other sources (Bonnefoy-Claudet et al., 2009; De Guevara et al., 2022; Talha Qadri et al., 2015). Special physical parameters such as the fundamental site frequency, amplification factor, sedimentary thickness, and vulnerability index vary from place to place due to variations in local geology; hence, estimating these parameters from the ambient noise recordings aids in site response analysis. These site-specific parameters give engineers and geoscientists an idea of just how much the soil can trap and amplify the seismic wave during an actual seismic event. One of the most effective methods used to achieve this is the horizontal-to-vertical spectral ratio (HVSR) analysis of ambient noise (Bonnefoy-Claudet et al., 2009; Mundepi et al., 2015; Nakamura et al., 2000).

The horizontal-to-vertical spectral ratio (HVSR) was initially presented by Nogoshi and Igarashi, but later developed by Nakamura and has proved to be a simple and reliable way of estimating local site effects over the years (Akkaya and Özvan, 2019; Bonnefoy-Claudet et al., 2009; Molnar et al., 2007; Talha Qadri et al., 2015). The technique has been reviewed in depth by the SESAME (Site Effect Assessment Using Ambient Excitation) project (Marcellini, 2006). The project proposed a comprehensive list of guidelines for effective measures to take when using the method and has since been applied in several densely populated and low-to-moderate seismic areas for earthquake engineering purposes with success (Onyebueke et al., 2017; Vella et al., 2013). The technique is an experimental procedure used to evaluate some characteristics of soft sediments, like the fundamental site frequency and amplification factor which are mostly adopted in microzonation investigations. Just like any other geophysical method, the HVSR technique is not absolute and should be used together with other methods to fully characterize the complexities of soft sediments (Marcellini, 2006). Particularly, the HVSR technique underestimates the amplification factor to an extent but gives a reliable estimate of the fundamental site frequency (Field and Jacob, 1993; Parolai, 2012). Sediment thickness can be calculated from ambient noise using the HVSR technique. Sediment thickness is an equally important parameter in earthquake engineering and construction work as it plays a crucial role in the stability of building foundations (Bard, 1998; Field and Jacob, 1993; Tian et al., 2019). The soil vulnerability index can also be estimated using ambient noise measurements (Nakamura, 1997). A seismic soil vulnerability index assesses and quantifies the vulnerability of regions or buildings to earthquake hazards. The spectral ratios of ambient noise simultaneously measured on structures and their foundation ground surface can be used to assess the seismic response characteristics of buildings (Nakamura, 1997). Extensive research has shown that this simple and affordable approach based on the HVSR analysis of ambient noise shows a good correlation with strong motion analysis such as earthquakes (Ullah and Prado, 2017). All these parameters are valuable tools for urban planning, risk reduction, and preparing for disasters in seismically active places. It helps

authorities prioritize resources, implement building codes and construction standards, and plan emergency response strategies.

Active artificial seismic sources such as explosions or heavy mass drops are not appropriate in heavily populated regions for strong ground motion analysis (Chen et al., 2009). In the case of the Greater Accra Metropolitan Area (GAMA), the HVSR on ambient noise approach is the most suitable method for site effect estimation because strong earthquakes very rarely occur and also there are few permanent seismographs installed for adequate ground motion monitoring (Amponsah et al., 2009). Even though the public's general perception is that seismic risk is negligible, historic records and recent tremors only indicate that the area is still seismically active and requires the needed attention. The June 22, 1939 earthquake with an estimated magnitude of 6.4 is considered the most destructive as it struck the capital city Accra causing significant damage to infrastructure, including buildings, roads, and water systems, and also resulted in the loss of 17 lives and injured about 133 people. A few tremors in recent years have served as a reminder of the region's susceptibility to seismic events. These include the November 12, 2023 tremor in Accra with a magnitude of 3.6 and a series of tremors on December 12, 2022 which included one with a magnitude of 3.5. The recent increasing rate of urbanization in the GAMA due to the centralization of countless industries within it has caused a dramatic increase in building density since the last destructive earthquake. Buildings in the area are generally not constructed to be resilient and to withstand earthquake shocks (Ahulu et al., 2018; Ayetey and Andoh, 1988; Nortey et al., 2018). With most recent structures being mounted on different geologic units which are yet to be investigated for their site effect conditions.

It is therefore a crucial task for urban regions, such as the GAMA, to have a concrete and appropriate plan of seismic hazard mitigation because it is at a high risk of earthquake destruction even though it is in a relatively low-to-moderate risk zone (Irinyemi et al., 2022; Kadiri and Amponsah, 2021; Meghraoui et al., 2019). Infrastructure engineers, town planners, and emergency response units including the National Disaster Management Organization (NADMO) are constantly seeking high-resolution data and accurate geotechnical information on how to assess seismic damage, design infrastructure to withstand earthquakes, and plan for and respond to emergencies. This research arises out of the need to improve and add to the scientific and geotechnical knowledge concerning seismic risk to buildings in the GAMA as well as estimate potential risk zones for future buildings in the area using the horizontal-to-vertical spectral ratio approach.

Objectives and Significance

Despite the Greater Accra Metropolitan Area (GAMA) recording damaging earthquakes in the past and tremors in recent times, detailed information on how local soil characteristics influence seismic response across the region remains limited.

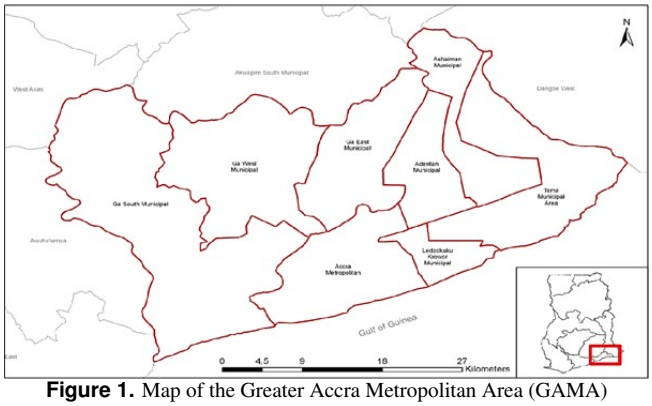

Figure 1. Map of the Greater Accra Metropolitan Area (GAMA)

Buildings continue to be constructed over a diverse range of geological units, mainly due to rapid urban growth. Many of these units have not been thoroughly assessed for their site response characteristics. This gap presents the importance of site effect analysis for effective seismic hazard mitigation, urban planning, and earthquake-resistant design in the region. The primary objective is to characterise site effects and assess seismic vulnerability within GAMA by applying the horizontal-to-vertical spectral ratio (HVSR) to ambient noise recordings. The analysis will review key site response parameters, including the fundamental site frequency and its corresponding amplification factor, sedimentary thickness, and seismic vulnerability index at the selected sites across the GAMA.

The results and findings from the study can inform land-use planning, guide safer building design, and contribute to strategies that aim to reduce earthquake-related risk in GAMA by highlighting zones of increased seismic vulnerability.

Study Area

The Greater Accra Metropolitan Area (GAMA)

The Greater Accra Metropolitan Area (GAMA) covers the majority of the Greater Accra Region in Ghana, encompassing Accra Metropolis, Ashaiman, Tema Metropolis, Ga East, Ga South, Ga West, Adenta, Ledzokuku Krowor and others as shown in Figure 1 (Nortey et al., 2018; Owusu, 2012). The size of the GAMA is approximately 1,550.37 km^2 land area and is bounded between latitudes 5°45′0″ N and 5°25′0″ N and longitudes 0°30′0″ W and 0°05′0″ E along the Atlantic coast of Ghana.

The area is mainly undulating in the east, grading into the Accra plains. There are recognisable high ranges, such as the Akwapim ranges, trending from northeast to southwest (Ahulu et al., 2018; Amponsah et al., 2009; Ayetey and Andoh, 1988; Nortey et al., 2018). There are a few isolated hills and rock outcrops scattered across the region, which range from flat to gently undulating slopes rising to 75 meters at the foothills (Addae and Oppelt, 2019).

The GAMA has experienced a constantly increasing rate of urbanization over the past decades from a group of fishing communities and has developed into Ghana's economic centre,

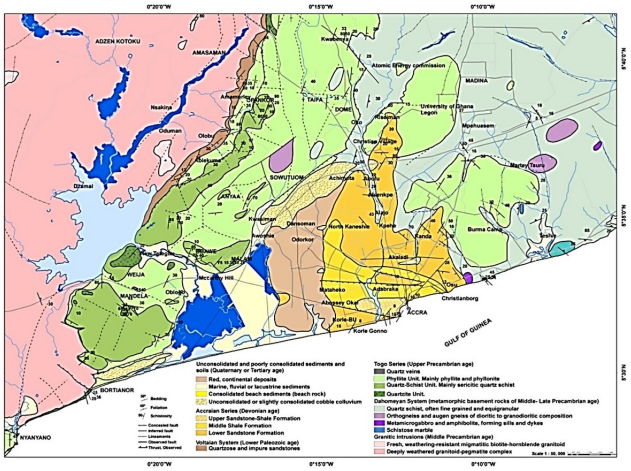

Figure 2. Geological Map of the GAMA (Dawood et al., 2012)

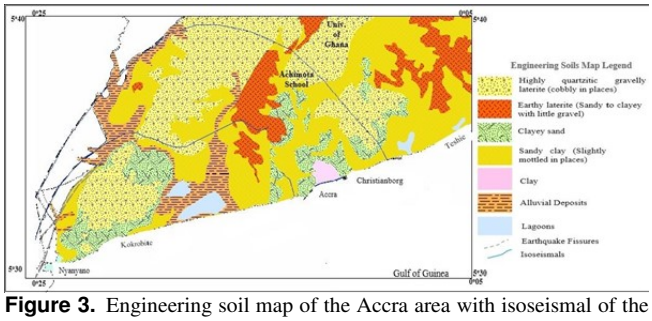

Figure 3. Engineering soil map of the Accra area with isoseismal of the 1939 Earthquake. Digitized and modified after Nortey et al. (2018)

attracting investors from all over the country and the world. The GAMA is currently the most economically industrialized region in Ghana (Allotey et al., 2010). According to the report by Addae and Oppelt (2019), Nortey et al. (2018), and Imoro Musah et al. (2020), it has a population that approximates to about five million and is expected to double in 20 years, making it the largest metropolis by population in Ghana.

Geological Setting

The geological makeup of Southern Ghana, as indicated in Figure 2, is fairly simple. According to Ayetey and Andoh (1988), the basement rocks to the east of the Akwapim hills are generally of the Dahomeyide belt metamorphosed Precambrian sediments which are predominantly hard, foliated, and folded gneisses. The Dahomeyide belt are overlain with the much younger Togo series rocks which are hard quartzites or recrystallized sandstones. The Togo series is characterized by interbedded quartz and mica schist which are folded, faulted, and mainly trend northeast to southwest. Rocks of the Accraian formation underlie most of the central part of the study area. The Accraian formation consists mainly of Devonian shales and interbedded sandstones.

Engineering soil distribution concerning bedrock topography

Residual soils form a complex spatial distribution, and the process is generally controlled by bedrock, drainage, and topography. These soils are made of patches of lateritic soils on higher ground and sands and clays on lower ground, primarily depending on whether the bedrock is made up of sandstones, quartzites, or shales (Ayetey and Andoh, 1988; Nortey et al., 2018). Figure 3 represents a map developed using data from boreholes in the Accra area that were drilled for site investigations (Ayetey and Andoh, 1988).

In low-lying areas, the Accraian interbedded sandstone and shale deposits typically produce fine to coarse sands, which become silty to clayey where shales are interbedded. However, on higher terrains with satisfactory drainage, lateritic soils that range from sandy to gravelly are more dominant. The shale series normally forms the clays. In low-lying places, the Togo series often produces fine to coarse sand that ranges from gravelly laterites to highly quarzitic cobbly to gravelly laterites on high ground, with the schist zones producing clayey to silty sands. The Dahomeyan rocks undergo weathering to form residual soils with thick clay and silty-sandy clay in river channels and valleys. Generally, alluvial deposits are of clayey to silty material (Ayetey and Andoh, 1988; Junner, 1941; Kwayisi et al., 2023). The depth and products of weathering of these formations can be used to determine seismic risk in these areas (Amponsah et al., 2009, 2008). These soft residual soils may amplify seismic energy rendering such areas highly vulnerable and at risk of earthquake damage.

Seismotectonic setting of the GAMA

Southern Ghana is known for being the most seismically active part of the country. Three separate tectonic zones, with varying tectonic features, make up southern Ghana's seismotectonic setting and its offshore area. These tectonic zones are the Akwapim fault zones, the Romanche fracture zone, and faults in the shelf and coast, which are mainly comprised of the Coastal boundary fault (Asare-Bediako et al., 2024). The majority of recent earthquakes and tremors have occurred along the Akwapim fault zones and the Coastal boundary fault (Ahulu et al., 2018).

Akwapim Fault Zones

This is a system of thrust faults trending from southwest to northeastwards through Kpong, Ho, and into Togo and Benin. The fault zone is outlined by the Western Boundary Fault (WBF) and the Eastern Boundary Fault as shown in Figure 4. In recent years, the zone has undergone a block-tectonic style of deformation that has resulted in several normal faults developing (Ahulu et al., 2018; Amponsah et al., 2012). Some faults in this zone include the Akwapim fault and the Nyanyanu fault.

Faults in the coastal area and shelf

The 1939 earthquake sparked a series of research into understanding the seismotectonic make up of Southern Ghana. Analysis of knowledge on land geology and interpretation of seismic reflection survey of the continental shelf led to the discovery of the presence of some faults in the area as per

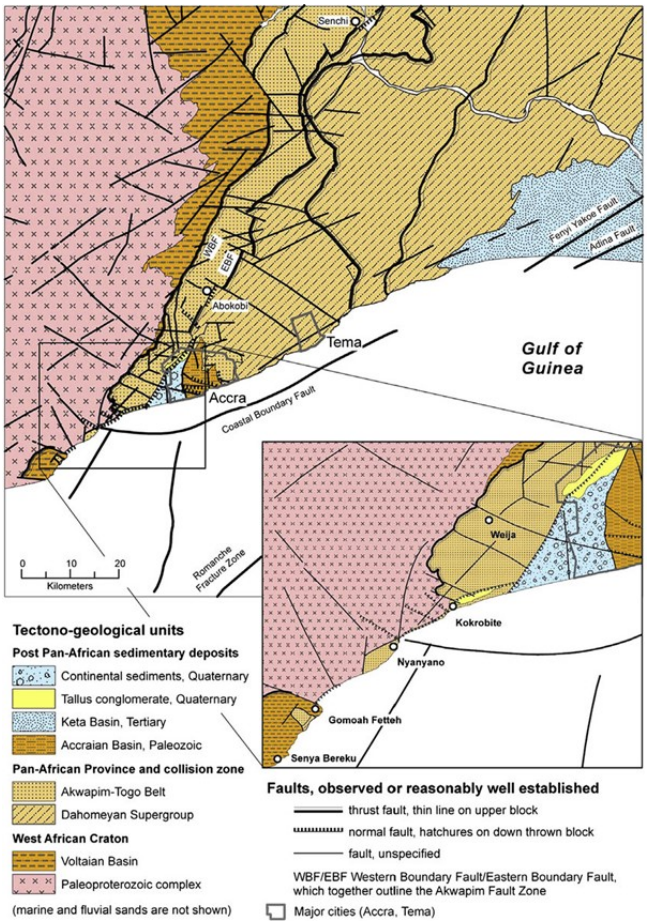

Figure 4. Neotectonics and Geological sketch map of South-East Ghana (Amponsah et al., 2012)

Blundell (1976). The Coastal Boundary Fault is the most prominent normal fault in the shelf (Amponsah et al., 2012). It trends east-west as shown in Figure 4. It intersects the Akwapim fault just to the west of Accra. Blundell (1976) explained that the Coastal Boundary Fault forms the northern margin of the Keta Basin. Other faults in this zone that are believed to be active include the Fenyi-Yakoe and Adina faults (Amponsah et al., 2012).

Romanche Fracture Zone

Figure 4 shows the Romanche Fracture Zone (RFZ), an offshore fault system that runs almost parallel to the coastline. It is an inactive transform fault of the Mid-Atlantic Ridge which differentiates the continental crust from the oceanic crust (Attoh et al., 2005).

Neotectonics of Southern Ghana

A study by Amponsah et al. (2012) on the tectonic-structural evolution of Southeast Ghana, made clear the fact that the forces that caused deformation during the Pan-African orogenesis no longer exist in the present day. However, discoveries of high-to-moderate-angle neo-tectonic normal faults indicate that tectonic movement is still ongoing (Amponsah et al., 2012). Such faults are believed to be utilizing weakened zones and hence may mimic the older Pan-African fault directions. Neo-tectonic faulting is believed to be greatly involved in modern-day seismic activity in the area. The study predicts that there could be more such faults existing than known either from topographic analysis or interpretation of drill holes in the Akwapim Togo belt. The reason is that there is usually an absence of contrasting lithologies, and thick soil cover keeping them hidden.

Ghana's continental margin subsides, exerting a shearing force that is believed to be the resulting factor of the occurrence of the numerous neo-tectonic normal faults in the coastal area and shelf. Lithological heterogeneities in the crust and pre-existing structures are also contributing factors to the formation of such normal faults (Amponsah et al., 2012). Such faults can be located in areas such as Abokobi, Nyanyano-Kokrobite, and to the West of Accra, the southernmost section of the EBF as shown in Figure 4.

Materials and Methods

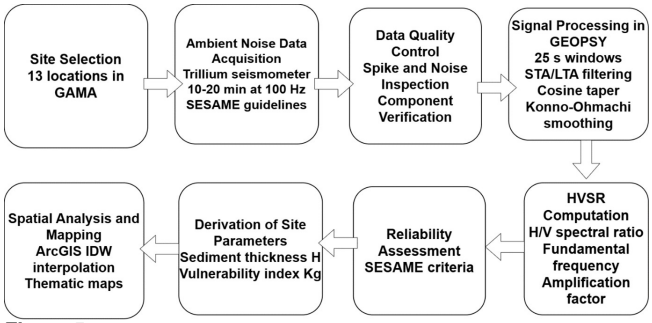

Figure 5. Flowchart illustrating the sequence of data acquisition, processing, and analysis workflow adopted in this study

Data Acquisition and Analysis

The current study was carried out by collecting ambient noise data from 13 different points using the *Taurus Trillium Nanometric* as shown in Figure 6. The Trillium seismometer was placed in a stable and secure location on the ground at each site to achieve effective soil-to-sensor connections for each reading and away from any artificial vibrations like heavy machinery. The ground was cleared of debris, vegetation, and any loose material. The three adjustable height feet and the levelling bubble work together to level and centre the sensor precisely. Proper alignment was also ensured by positioning the sensor such that the north-south vertically scribed marks and the north-south case-top guide all point in the direction of the North using a compass (Figure 7). The system's clock was then synchronized with GPS time. After this, the seismometer was protected from adverse weather conditions such as extreme temperature or rain using the insulated seismometer cover (Figure 6). A continual recording of ambient noise for about 10 to 20 minutes at a sample rate of 100 Hz was made taking into account the guidelines from the SESAME project (Marcellini, 2006).

Processing of the data was done using the GEOPSY software which also allowed for calculation of the H/V ratio after the

Figure 6. Taurus Trillium Nanometric. (1) Nanometric Trillium seismometer (2) Insulating seismometer base (3) Insulated seismometer cover (4) GPS antenna (5) Nanometric Taurus datalogger (6) battery

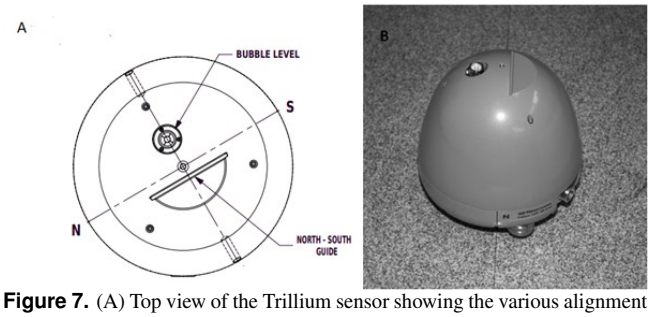

Figure 7. (A) Top view of the Trillium sensor showing the various alignment and leveling features; bubble level, north-south scribed vertical lines, and case-top guide (B) An illustration of the north-south scribed vertical being aligned to a north-south trending

recordings were downloaded from the seismometer. The ambient noise recordings were then imported into the software and reviewed for any obvious issues such as gaps, spikes, or periods of non-seismic noise to ensure good data quality. The orientations of the components (N-S, E-W, Z) are also reviewed to ensure that they are correctly recognized by the software. As shown in Figure 8, the recordings were then divided into low-noise 25-second windows using the short-term average (STA)/long-term average (LTA) anti-trigger. STA was given a value of 2 s while LTA was given a value of 30 s with min STA/LTA and max STA/LTA thresholds of 0.2 and 2.5 respectively. Cosine taper is applied at two ends of the selected signal window while processing ambient noise recording to overcome abrupt discontinuities that greatly affect the Fourier spectrum (Chatelain and Guillier, 2013). Konno-Ohmachi smoothing option was applied to smoothen the Fourier amplitude spectra along with the Cosine taper. The 'squared average' option was used to combine the Fourier spectra of the horizontal components (Figure 8). These processing procedures were completed following the instructions in the Geopsy manual (Wathelet et al., 2020). The H/V is finally determined and the fundamental frequency, f_o and its corresponding amplification factor, A_o are deduced from it.

Data reliability was checked based on the conditions proposed by Marcellini (2006) which includes, $f_o > \frac{10}{L_w}$, $n_c(f_o) > 200$,

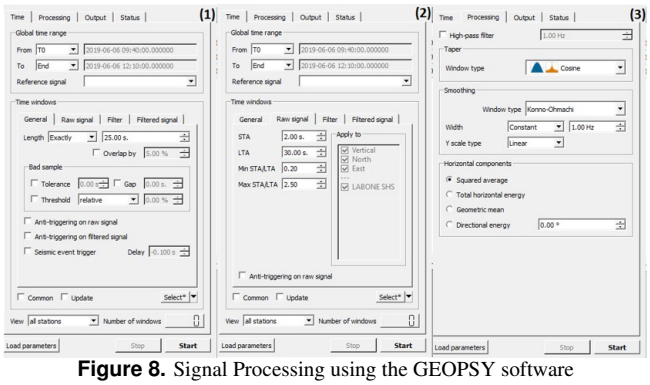

Figure 8. Signal Processing using the GEOPSY software

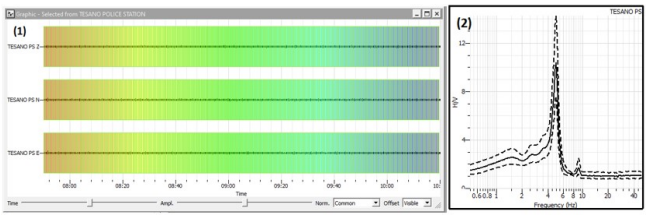

Figure 9. (A) Window selection for three components of the ambient recordings. (B) A sample of the H/V curve after the processing

(where $n_c = n_w \times L_w \times f_o$) and $A_o > 2$ (L_w = window length, f_o = H/V peak frequency, n_w = the number of windows selected for the average H/V curve, n_c = the number of significant cycles, A_o = H/V peak amplitude at frequency f_o). The parameters are then used to estimate the thickness H of the sedimentary layer and the vulnerability index of the site. To illustrate the spatial variation of the derived site parameters, interpolation using the Inverse Distance Weighted method was performed in ArcGIS software. This was selected ahead of other common interpolation techniques, such as kriging and spline methods because they require a dense and uniformly distributed dataset to produce reliable results. Given the limited number of measurement points and their uneven spatial distribution within the study area, the IDW method was considered more appropriate for this study. This was carried out by importing a tabulation of the results with columns for coordinates into the ArcGIS software. These measurements were georeferenced. Separate interpolated surfaces were generated for the resonance frequency, amplification factor, sedimentary thickness and the vulnerability index. The Aburi site was not included in the spatial interpolation because the HVSR peak did not satisfy the SESAME reliability criterion (amplification < 2). The H/V curve at this location is nearly flat, which is typical of hard rock sites with little impedance contrast. Although it was excluded from the interpolation, the Aburi record is still useful for interpreting site conditions and serves as a reference for the harder ground response in the study.

Results and Discussions

Results

HVSR analysis was carried out using ambient noise recordings collected at 13 locations across the study area. However,

Table 1. Reliability of frequency peaks/curves based on parameters defined by guidelines modified by Marcellini (2006)

Station	Lat	Long	f_o	$A_o > 2$	$f_o > \frac{10}{l_w}$	n_w	$n_c(f_o) > 200$	Comment
Aburi	5.84	-0.18	0.73	1.66	0.4	23	420.06	UNRELIABLE
Anyaa DL	5.59	-0.29	6.75	3.13	0.4	23	3882.71	RELIABLE
Ayikuma	5.77	-0.18	11.00	2.34	0.4	23	6328.22	RELIABLE
LA C&W	5.58	-0.16	4.06	2.17	0.4	23	2331.62	RELIABLE
Labone SHS	5.56	-0.16	9.40	2.90	0.4	23	5404.31	RELIABLE
Lapaz	5.61	-0.25	11.02	2.02	0.4	23	6335.01	RELIABLE
NADMO HQ	5.58	-0.19	5.49	2.20	0.4	23	3156.08	RELIABLE
NLN Bus Terminal	5.69	-0.16	8.47	2.70	0.4	23	4869.84	RELIABLE
Odorkor SDA	5.58	-0.26	10.12	2.06	0.4	23	5819.86	RELIABLE
Otinshie	5.66	-0.15	6.44	3.11	0.4	23	3703.56	RELIABLE
Pantang HOSP.	5.72	-0.19	7.33	2.49	0.4	23	4212.80	RELIABLE
Social Welfare	5.68	-0.16	7.79	2.02	0.4	23	4483.46	RELIABLE
Tesano PS	5.60	-0.22	4.95	9.94	0.4	23	2850.06	RELIABLE

Note: l_w = window length, f_o = H/V peak frequency, n_w = the number of windows selected for the average H/V curve, n_c = the number of significant cycles ($n_c = n_w \times L_w \times f_o$), A_o = H/V peak amplitude at frequency f_o.

Table 2. 13 sites of data acquisition along with corresponding fundamental frequencies f_o, amplification factors A_o, thicknesses H and the vulnerability index K_g

Station	Latitude	Longitude	f_o	A_o	H	K_g (A_o^2/f_o)
Aburi	5.84	-0.18	0.73	1.66	175.75	3.81
Anyaa DL	5.59	-0.29	6.75	3.13	5.58	1.45
Ayikuma	5.77	-0.18	11.00	2.34	2.62	0.49
LA C&W	5.58	-0.16	4.06	2.17	12.31	1.16
Labone SHS	5.56	-0.16	9.40	2.90	3.34	0.87
Lapaz	5.61	-0.25	11.02	2.02	2.61	0.37
NADMO HQ	5.58	-0.19	5.49	2.20	7.69	0.88
NLN Bus Terminal	5.69	-0.16	8.47	2.70	3.92	0.84
Odorkor SDA	5.58	-0.26	10.12	2.06	2.98	0.42
Otinshie	5.66	-0.145	6.44	3.11	6.00	1.50
Pantang HOSP.	5.72	-0.19	7.33	2.49	4.91	0.84
Social Welfare	5.67	-0.16	7.79	2.03	4.46	0.52
Tesano PS	5.60	-0.22	4.95	9.94	9.02	20.00

Note: f_o = fundamental site frequency (Hz); A_o = amplification factor; H = sedimentary thickness (m); K_g = seismic vulnerability index.

the Aburi site did not meet the SESAME reliability criteria and was therefore excluded from the spatial interpolation. The interpolated maps presented in this study are therefore based on the remaining 12 reliable measurement sites. Table 1 represents the results obtained for the fundamental site frequency and its corresponding amplification factor as well as the data reliability check as proposed by the SESAME project (Marcellini, 2006). The reading from Aburi was rendered unreliable because the amplification factor is less than 2. However, the flat H/V curve is consistent with hard bedrock conditions. Table 2 shows the estimations of sedimentary thickness, H and the vulnerability index, K_g of each site from Table 1.

Fundamental site frequency f_o and Alluvium thickness estimates

The fundamental site frequency values obtained after the analysis of the recordings from the 13 sites are shown in Table 2. The values ranged from 0.73 Hz to 11.00 Hz. The thickness over the area also ranged from 2.61 m to 175.75 m. The least fundamental site frequency value occurred at Aburi with a value of 0.73 Hz, while Lapaz recorded the highest value of 11.02 Hz. The highest f_o corresponds with the lowest thickness and the lowest f_o corresponds to the highest thickness.

Amplification factor A_o and Alluvium thickness estimates

The amplification factor from the HVSR analysis ranges from 1.6 to 10.0. The least amplification recorded corresponds

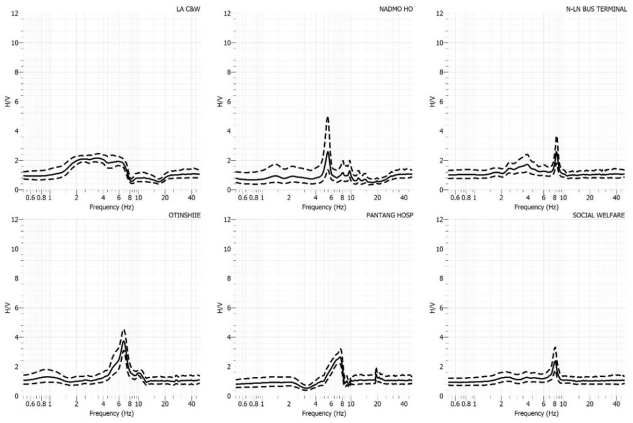

Figure 10. H/V curves for various sites

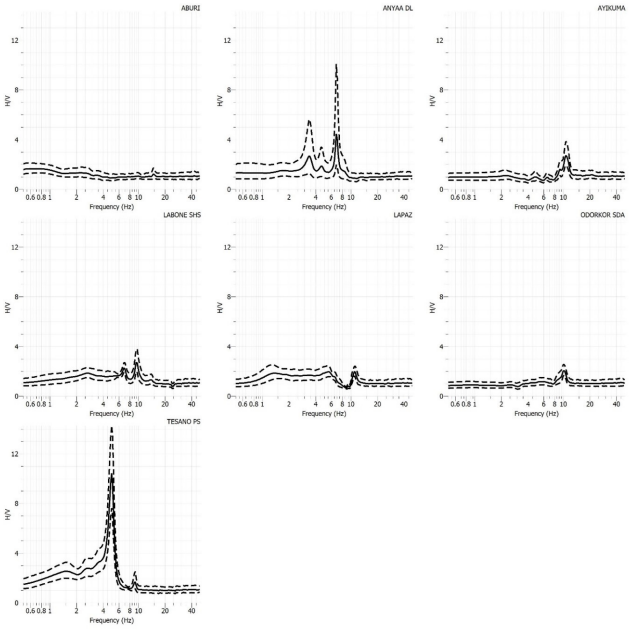

Figure 11. H/V curves for the various sites

to the highest alluvium thickness. The highest estimated amplification factor, however, does not correspond to the maximum alluvium thickness. The thickness estimated at Tesano PS is 9.00 m which is comparatively deep (Table 2).

Vulnerability Index, K_g (A_o^2/f_o)

The values from the estimation of the vulnerability indices range from 0.37 to 20.00. Tesano PS showed the highest reading of 20.00. Lapaz recorded the lowest value of 0.37 (Table 2).

Discussion

Implications of H/V curves and f_o concerning site characteristics

Most instances in literature indicate that H/V curves for soft soils have noticeable peaks while rocky sites appear nearly flat (Bonnefoy-Claudet et al., 2009; Bour et al., 1998; Fäh et al., 1997; Lermo and Chavez-Garcia, 1993). The presence of peaks suggests the possibility of amplification of seismic ground motion. The amplitude indicates the degree of amplification of the ground motion at the corresponding resonance frequency (Lermo and Chavez-Garcia, 1993). The curves obtained during the study include clear single peaks, multiple peaks, flat peaks, and broad peaks as shown in Figures 10 and 11.

Clear Peaks

Clear and distinct curves correspond to the natural frequencies of the subsurface layers. A clear single peak has been exhibited in some sites such as the ones labelled Tesano PS and Otinshie among others shown in Figures 10 and 11. Such curves may be an indication of a single layer that presents a large impedance contrast and is usually likely to amplify ground motion. Higher peaks correspond to higher velocities, which may signify softer soils overlying a more rigid or denser rock (Bonnefoy-Claudet et al., 2009; Cruz et al., 1993; SESAME (Site EffectS Assessment using AMbient Excitations), 2004). According to Bonnefoy-Claudet et al. (2009) and Lermo and Chavez-Garcia (1993), softer and less dense materials tend to have lower resonance frequencies and corresponding higher amplification, while stiffer and denser materials have higher resonance frequencies and lower amplification. Tesano PS appears to be the most vulnerable according to this analysis.

Multiple Peaks

The presence of multiple clear peaks may be an indication of the presence of multiple surface layers with varying shear wave velocities. Each peak represents the fundamental frequency of distinct geotechnical layers (Lermo and Chavez-Garcia, 1993). The curve from Anyaa DL shows the most prominent double peaks (Figure 11).

Broad Peaks

Broad peaks may also be an indication of multiple layers with slightly different fundamental frequencies. It may also be an indication that amplification may occur over a large range of frequencies which are less distinct than the sharp multiple peaks (Lermo and Chavez-Garcia, 1993). LA C&W demonstrated a broad peak (Figure 10).

Flat Curves

A flat curve may reflect a consistent site response that is less susceptible to amplification or resonance effects, it is typically regarded as being advantageous for seismic resilience. Flat curves may be due to a lack of resonance, which suggests that there is an absence of an impedance contrast. It also suggests that the site is on solid bedrock. In effect, a uniform layer of soil extends over a range of depths (Lermo and Chavez-Garcia, 1993; SESAME (Site EffectS Assessment using AMbient Excitations), 2004). Aburi shows a flat curve. Although the Aburi site did not produce a reliable HVSR peak, the flat response is consistent with hard bedrock conditions. For this reason, it was excluded from the interpolation analysis but retained in the discussion as a reference for the harder ground

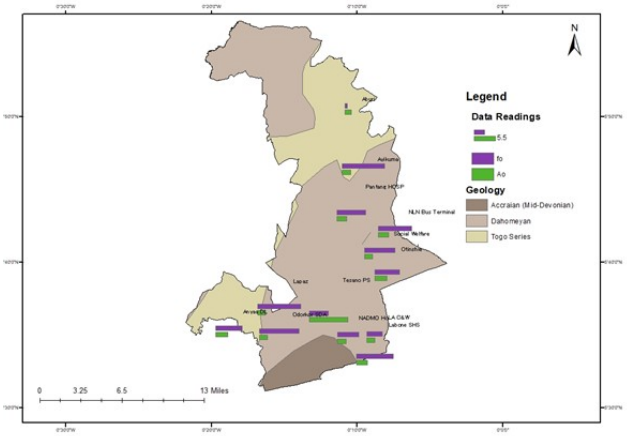

Figure 12. Site Response Map for selected sites in the GAMA

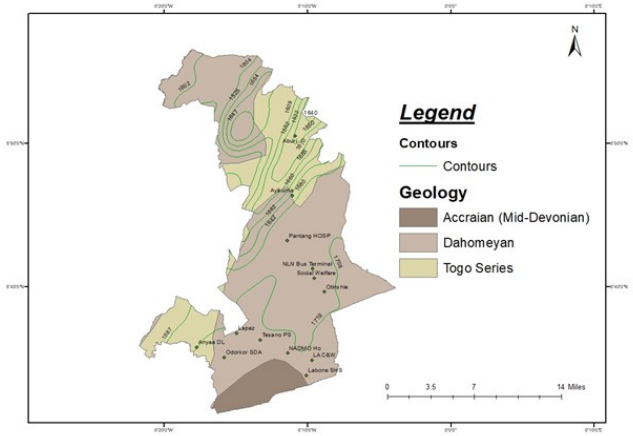

Figure 13. Site Response Map for selected sites in the GAMA showing contours

conditions within the study area (Figure 11).

Characteristic response of different lithologies

The different lithologies appear to show varying responses to seismic motion based on their H/V curves. In Figures 12 and 13, the spatial variation of f_o and A_o has been shown on maps of the basement rocks of the GAMA. The length of the bars indicates the magnitude of the fundamental frequency and amplification factor recorded at the site. The site of most interest is the Tesano PS which appears to be the most vulnerable because it has a smaller fundamental frequency but high corresponding amplification indicating soft soils. Its H/V curve peak also supports this (Figure 11). Also, in Figure 14, the site in Tesano PS is on clayey sands.

The site in Aburi shows both the lowest fundamental frequencies and corresponding amplification. Since the curve and values correspond to a zero-impedance contrast site, further analysis suggests that the ambient noise recording at that site might have been made on a hard outcrop which could be a basement rock on high ground (Figure 13). Ayikuma is located just at the transition between the Togo and the Dahomeyide belts, and considering the contours, it appears to be on a relatively lower land. This may be the reason for the difference in site response there as there may be some settled shallow weathered rocks overlying the basement rock. Anyaa DL differs as its curve demonstrates distinct peaks suggesting a complex soil combination. Based on the modified residual soil map of parts of the GAMA, Anyaa DL is sited on a highly quarzitic gravelly laterite. The multiple peaks observed in Figure 11 are consistent with such heterogeneous ground conditions.

Most sites are distributed in the Dahomeyide belts, and those located in the central part of the study area exhibit fundamental site frequencies and amplification factors that vary only slightly across the area. Pantang HOSP, NLN Bus Terminal, Social Welfare, and Otinshie have close fundamental site frequencies and their corresponding amplification. In Figure 10, they all show similar curves.

Odorkor SDA, NADMO HQ, Lapaz, LA C&W, and Labone SHS sites show some complexities with varying curves. Odorkor SDA and the Lapaz site showed almost similar curves and close values. They are both found on the earthy laterite which is clayey with little gravel in general. The site from NADMO HQ produced a single distinct peak with smaller peaks; in Figure 14 it is at the transition between highly quarzitic gravelly laterite and sandy clay. It may contain soils from both sides, explaining the peaks on the curve (Figure 10). LA C&W is located also on highly quarzitic gravelly laterite but produced a broad peaked curve suggesting multiple layers of close fundamental frequencies. Labone SHS site may contain residual soils from the clayey sands and sandy clays resulting in small but distinct peaks on the curve.

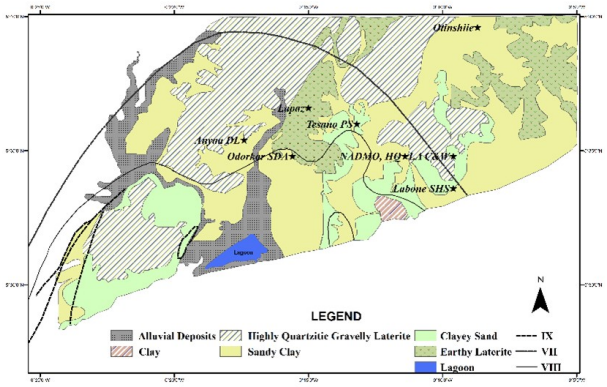

Figure 14. Engineering soils of some parts of the GAMA where data was recorded (modified after Nortey et al. (2018))

Implication of vulnerability index K_g values

The vulnerability index estimate is an important parameter that is employed to calculate the levels of rock solidity and rock structure characteristics (Huang and Tseng, 2002). Areas with high values are considered to have weak structures and hence soft soils. During earthquakes, such soils can be moved easily by the shaking. Tesano PS recorded the highest value and may be susceptible to serious damage during earthquakes. Lapaz recorded the lowest value among the sites, indicating comparatively lower susceptibility to seismic am-

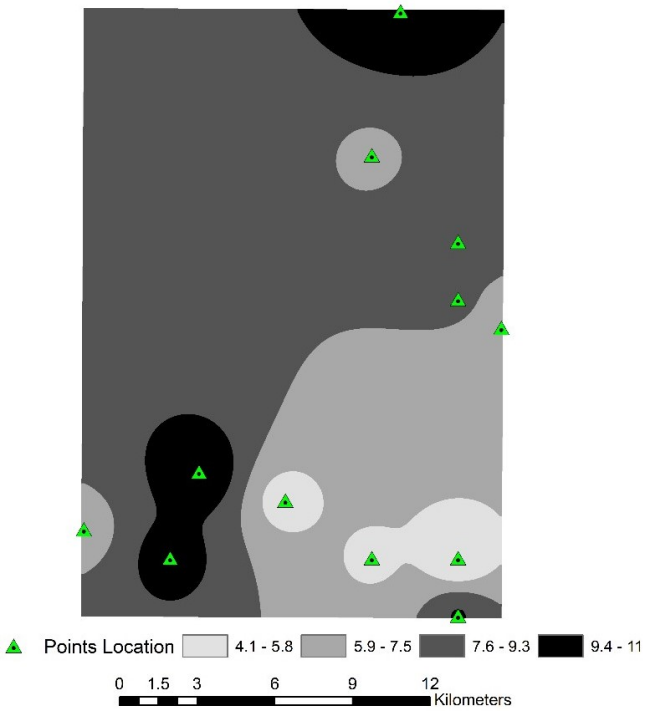

Figure 15. Interpolated map showing the spatial distribution of the fundamental site frequency (f_o) across the study area based on the 12 reliable measurement sites

plification. The low value suggests a relatively more stable ground condition as compared to the other sites.

Interpolation of obtained parameters

The spatial distribution of the derived site parameters was estimated using the Inverse Distance Weighted (IDW) interpolation method in ArcMap. Because the Aburi measurement did not satisfy the reliability criteria, only the remaining 12 reliable sites were used for generating the interpolated surfaces. The interpolation was performed using a power value of 2 with a variable search radius that considered all available measurement points. A grid cell size of approximately 200 m was used to produce smooth spatial surfaces for regional interpretation. The study area has been divided into four different zones in terms of fundamental frequency f_o, amplification factor A_o, sedimentary thickness H, and vulnerability index K_g.

The interpolated map of the fundamental frequency (f_o) shows clear spatial variations across the study area. Lower frequency values occur in areas such as Tesano PS and parts of central Accra, suggesting thicker sedimentary layers that may favour the amplification of ground motion. Higher frequency values appear in areas where the subsurface materials are relatively shallow or more competent. The variations likely reflect differences in sediment thickness and local geological conditions across the area.

The amplification factor (A_o) map highlights differences in the level of ground-motion amplification across the study area. Higher amplification values are observed around Tesano PS, indicating the presence of softer sedimentary materials that

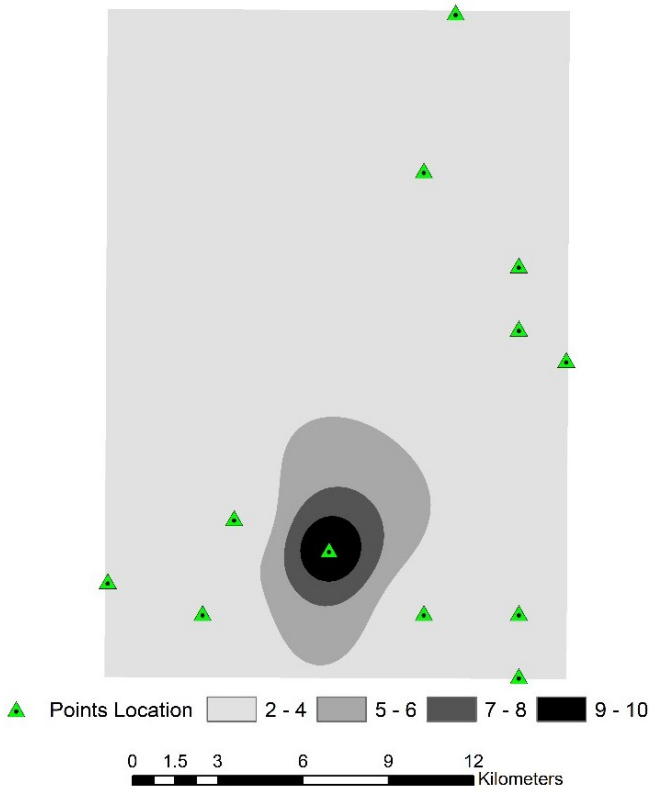

Figure 16. Interpolated map showing the spatial distribution of the amplification factor (A_o) across the study area based on the 12 reliable measurement sites

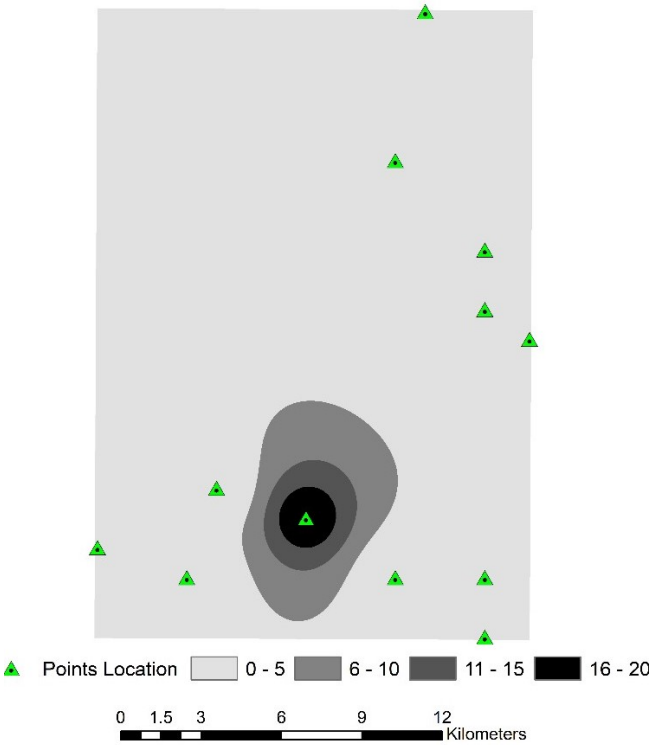

Figure 17. Interpolated map showing the spatial distribution of the vulnerability index (K_g) across the study area based on the 12 reliable measurement sites

can enhance seismic wave amplitudes. In contrast, lower amplification values occur in areas where the subsurface is

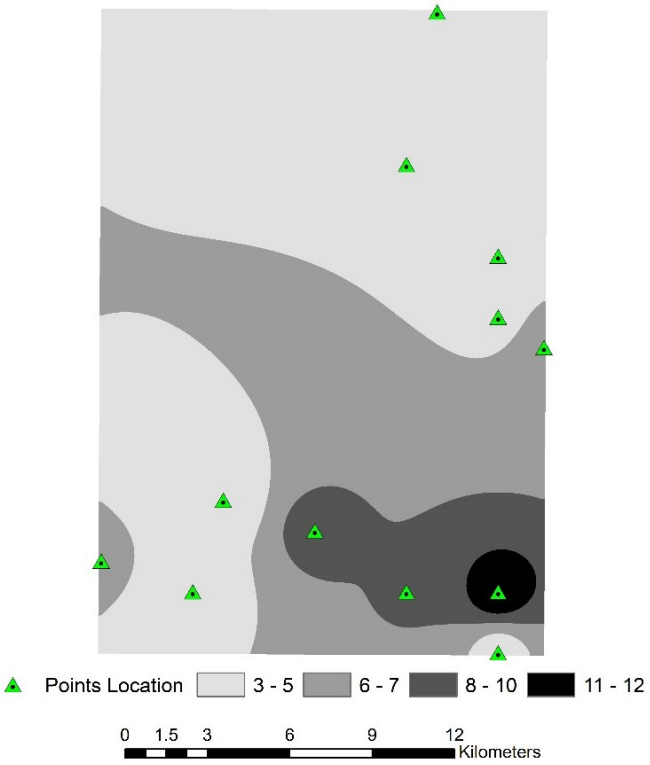

Figure 18. Interpolated Map showing the spatial distribution of the sedimentary thickness (H) across the study area based on the 12 reliable measurement sites

relatively stiffer. The pattern suggests that some parts of the city may experience stronger shaking during seismic events than others.

The spatial distribution of the vulnerability index (K_g) reflects the combined influence of the fundamental frequency and amplification factor. Higher K_g values tend to occur in areas where both amplification and sediment thickness are relatively high, indicating locations that may be more susceptible to seismic damage. Lower values are associated with areas where the ground conditions are comparatively stable and less likely to produce strong site effects.

The sediment thickness (H) map provides an estimate of the depth of unconsolidated materials across the study area. Thicker sediments are generally associated with lower fundamental frequency values, indicating deeper sedimentary deposits. Conversely, thinner sediment cover corresponds to higher frequency responses, which may suggest shallower bedrock or more compact subsurface materials. The overall pattern is consistent with the variations observed in the other HVSR-derived parameters.

Taken together, the interpolated maps further reinforce the site-specific observations derived from the H/V curves. Areas characterised by clear and well-defined spectral peaks, such as the Tesano PS site, coincide with zones of low fundamental frequency, high amplification, and elevated soil vulnerability index on the interpolated surfaces. These spatial patterns indicate that sites exhibiting pronounced resonance behaviour are not isolated but form coherent zones of increased seismic response. As a result, the interpolated maps provide a spatial framework for extending point-based HVSR interpretations across the study area, supporting their use in engineering design, land-use planning, and earthquake risk mitigation.

Conclusion

The fundamental frequency, f_o, amplification factor, A_o, depth to bedrock H, and the vulnerability index K_g were estimated for 13 sites in the GAMA using the horizontal-to-vertical spectral ratio analysis of ambient noise. These estimates are important in assessing seismic risk in the study area. The interpretation of the H/V curve revealed four major patterns from the sites: clear single peaks, multiple peaks, broad and flat peaks. The peaks correspond to major differences in seismic responses. Aburi exhibited a flat H/V response with low amplification, consistent with hard bedrock conditions. Although the site did not yield a reliable HVSR peak for site effect estimation, the flat spectral response itself is meaningful and suggests minimal impedance contrast at the site. For this reason, Aburi is not included in the interpolation but provides a useful reference for comparison with the amplified sites. Tesano PS revealed a single clear peak and the highest amplification factor, indicating soft soils that are more vulnerable to destruction than those at the other sites. In contrast, Lapaz revealed no pronounced H/V peak and a low amplification factor among the analyzed sites, indicating comparatively stiffer ground conditions. The vulnerability index estimates are in clear agreement with this. There is evidence to support intuitive theories that higher seismic risk exists in areas where clay layers are present. The remaining sites exhibit intermediate ground conditions, falling between the soft soils at Tesano PS and the hard ground response at Aburi. They showed broad and multiple peaks which also inform about the seismic properties of the sites. Estimating such site effect parameters is the first essential stage in the mitigation of seismic hazards. To develop effective mitigation techniques to lessen the effects and reduce the damages caused by this natural hazard, policymakers and disaster management authorities will find the study's findings to be of great value. Clear peaks, when considered alongside the spatial patterns observed in the interpolated maps, provide a useful basis for inferring seismic behavior and help inform engineering decisions to mitigate earthquake-related risk.

References

Addae, B. and Oppelt, N. (2019). Land-Use/Land-Cover Change Analysis and Urban Growth Modelling in the Greater Accra Metropolitan Area (GAMA), Ghana. *Urban Science*, 3(1):26. https://doi.org/10.3390/urbansci3010026.

Ahulu, S. T., Danuor, S. K., and Asiedu, D. K. (2018). Probabilistic seismic hazard assessment of southern part of Ghana. In *Geophysical Research Abstracts*, volume 20, pages 539–557.

Akkaya, I. and Özvan, A. (2019). Site characterization in the Van settlement (Eastern Turkey) using surface waves and HVSR microtremor methods. *Journal of Applied Geophysics*, 160:157–170. https://doi.org/10.1016/j.jappgeo.2018.11.009.

Allotey, N. K., Arku, G., and Amponsah, P. E. (2010). Earthquake-disaster preparedness: The case of Accra. *International Journal of Disaster Resilience in the Built Environment*, 1(2):140–156. https://doi.org/10.1108/17595901011056613.

Amponsah, P., Leydecker, G., and Muff, R. (2012). Earthquake catalogue of Ghana for the time period 1615-2003 with special reference to the tectono-structural evolution of south-east Ghana. *Journal of African Earth Sciences*, 75:1–13. https://doi.org/10.1016/j.jafrearsci.2012.07.002.

Amponsah, P. E., Banoeng-Yakubo, B. K., Panza, G. F., and Vaccari, F. (2009). Deterministic seismic ground modelling of the Greater Accra Metropolitan Area, Southeastern Ghana. *South African Journal of Geology*, 112(3-4):317–328. https://doi.org/10.2113/gssajg.112.3-4.317.

Amponsah, P. E., Banoeng-Yakubo, B. K., Vaccari, F., and Panza, G. F. (2008). Seismic ground motion and hazard assessment of the Greater Accra Metropolitan Area, Southeastern Ghana. In *Proceedings of the 14th World Conference on Earthquake Engineering*, Beijing, China.

Anastasopoulos, I., Gazetas, G., Bransby, M. F., Davies, M. C. R., and El Nahas, A. (2007). Fault Rupture Propagation through Sand: Finite-Element Analysis and Validation through Centrifuge Experiments. *Journal of Geotechnical and Geoenvironmental Engineering*, 133(8):943–958. https://doi.org/10.1061/(asce)1090-0241(2007)133:8(943).

Asare-Bediako, B., Boateng, C. D., Opoku, N., Danuor, S. K., Arthur, L. N. B., and Anokwa, Y. M. (2024). Seismic activities in Ghana: A systematic review. *Heliyon*, 10(10):e31536. https://doi.org/10.1016/j.heliyon.2024.e31536.

Attoh, K., Brown, L., and Haenlein, J. (2005). The role of Pan-African structures in intraplate seismicity near the termination of the Romanche fracture zone, West Africa. *Journal of African Earth Sciences*, 43(5):549–555. https://doi.org/10.1016/j.jafrearsci.2005.09.006.

Ayetey, J. J. and Andoh, M. B. (1988). Earthquake Site Response Study of Accra Area, Ghana. Technical report, Geological Survey Department of Ghana.

Bard, P. (1998). Microtremor measurement: a tool for site effect estimation? In Irikura, K., Kudo, K., Okada, H., and Sasatami, T., editors, *The Effects of Surface Geology on Seismic Motion*, pages 1251–1279. Balkema.

Bard, P.-Y. (1994). Effects of surface geology on ground motion: Recent results and remaining issues. In *Proceedings of 10th European Conference on Earthquake Engineering*, pages 305–323.

Blundell, D. J. (1976). Active faults in West Africa. *Earth and Planetary Science Letters*, 31(2):287–290. https://doi.org/10.1016/0012-821X(76)90221-1.

Bonnefoy-Claudet, S., Baize, S., Bonilla, L. F., Berge-Thierry, C., Pasten, C., Campos, J., and Verdugo, R. (2009). Site effect evaluation in the basin of Santiago de Chile using ambient noise measurements. *Geophysical Journal International*, 176(3):925–937. https://doi.org/10.1111/j.1365-246X.2008.04020.x.

Bonnefoy-Claudet, S., Cotton, F., and Bard, P. Y. (2006). The nature of noise wavefield and its applications for site effects studies. A literature review. *Earth-Science Reviews*, 79(3–4):205–227. https://doi.org/10.1016/j.earscirev.2006.07.004.

Bour, M., Fouissac, D., Dominique, P., and Martin, C. (1998). On the use of microtremor recordings in seismic microzonation. *Soil Dynamics and Earthquake Engineering*, 17(7–8):465–474. https://doi.org/10.1016/S0267-7261(98)00014-1.

Bray, J. D. (2009). Designing buildings to accommodate earthquake surface fault rupture. In *Improving the Seismic Performance of Existing Buildings and Other Structures - Proc. 2009 ATC and SEI Conference*, pages 1269–1280. ASCE. https://doi.org/10.1061/41084(364)117.

Cadet, H., Macau, A., Benjumea, B., Bellmunt, F., and Figueras, S. (2011). From ambient noise recordings to site effect assessment: The case study of Barcelona microzonation. *Soil Dynamics and Earthquake Engineering*, 31(3):271–281. https://doi.org/10.1016/j.soildyn.2010.07.005.

Castellaro, S. and Mulargia, F. (2009). VS30 estimates using constrained H/V measurements. *Bulletin of the Seismological Society of America*, 99(2A):761–773. https://doi.org/10.1785/0120080179.

Chatelain, J. L. and Guillier, B. (2013). Reliable fundamental frequencies of soils and buildings down to 0.1 Hz obtained from ambient vibration recordings with a 4.5-Hz sensor. *Seismological Research Letters*, 84(2):199–209. https://doi.org/10.1785/0220120003.

Chen, Q. F., Liu, L. B., Wang, W. J., and Rohrbach, E. (2009). Site effects on earthquake ground motion based on microtremor measurements for metropolitan Beijing. *Chinese Science Bulletin*, 54(2):280–287. https://doi.org/10.1007/s11434-008-0422-2.

Chen, Y., Song, J., Zhong, S., Liu, Z., and Gao, W. (2021). Effect of destructive earthquake on the population-economy-space urbanization at county level-A Case Study on Dujiangyan county, China. *Sustainable Cities and Society*, 69:103345. https://doi.org/10.1016/j.scs.2021.103345.

Cruz, E., Riddell, R., and Midorikawa, S. (1993). A study of site amplification effects on ground motions in Santiago, Chile. *Tectonophysics*, 218(1–3):273–280. https://doi.org/10.1016/0040-1951(93)90273-M.

Damayanti, C. and Sismanto, S. (2021). The Relationship Between Amplification And Quality Factors of Seismic Waves In Surface Sediment Layer. In *Proceedings of the 1st International Conference on Physics and Applied Physics*, pages 2–7. EAI. https://doi.org/10.4108/eai.30-8-2021.2311500.

Dawood, A. M. A., Akiti, T. T., and Glover, E. T. (2012). Seismic refraction investigation at a radioactive waste disposal site. *Geoscience*, 2(2):7–13. https://doi.org/10.5923/j.geo.20120202.02.

De Guevara, J. L., Mojica, A., Ruíz, A., Ho, C. A., Rodríguez, K., Toral, J., and Fábrega, J. (2022). Ambient Noise H/V Spectral Ratio in Site Effect Estimation in La Mesa de Macaracas, Panama. *International Journal of Geophysics*, 2022:6171529. https://doi.org/10.1155/2022/6171529.

Fäh, D., Rüttener, E., Noack, T., and Kruspan, P. (1997). Microzonation of the city of Basel. *Journal of Seismology*, 1(1):87–102. https://doi.org/10.1023/A:1009774423900.

Field, E. and Jacob, K. (1993). The theoretical response of sedimentary layers to ambient seismic noise. *Geophysical Research Letters*, 20(24):2925–2928. https://doi.org/10.1029/93GL03038.

Gurler, E. D., Nakamura, Y., Saita, J., and Sato, T. (2000). Local site effect of mexico city based on microtremor measurement. In *12th World Conference on Earthquake Engineering*, Auckland, New Zealand.

Huang, H. C. and Tseng, Y. S. (2002). Characteristics of soil liquefaction using H/V of microtremors in Yuan-Lin area, Taiwan. *Terrestrial, Atmospheric and Oceanic Sciences*, 13(3):325–338. https://doi.org/10.3319/TAO.2002.13.3.325(CCE).

Hunter, J. A., Benjumea, B., Harris, J. B., Miller, R. D., Pullan, S. E., Burns, R. A., and Good, R. L. (2002). Surface and downhole shear wave seismic methods for thick soil site investigations. *Soil Dynamics and Earthquake Engineering*, 22(9–12):931–941. https://doi.org/10.1016/S0267-7261(02)00117-3.

Imoro Musah, B., Peng, L., and Xu, Y. (2020). Urban Congestion and Pollution: A Quest for Cogent Solutions for Accra City. *IOP Conference Series: Earth and Environmental Science*, 435:012026. https://doi.org/10.1088/1755-1315/435/1/012026.

Irinyemi, S. A., Lombardi, D., and Ahmad, S. M. (2022). Probabilistic seismic hazard assessment for West Africa region. *Georisk*, 16(2):315–329. https://doi.org/10.1080/17499518.2021.1952608.

Janusz, P., Perron, V., Knellwolf, C., and Fäh, D. (2022). Combining Earthquake Ground Motion and Ambient Vibration Recordings to Evaluate a Local High-Resolution Amplification Model—Insight From the Lucerne Area, Switzerland. *Frontiers in Earth Science*, 10:885724. https://doi.org/10.3389/feart.2022.885724.

Johnson, C. D. and Lane, J. W. (2016). Statistical comparison of methods for estimating sediment thickness from horizontal-to-vertical spectral ratio (HVSR) seismic methods: An example from Tylerville, Connecticut, USA. In *Proceedings of the Symposium on the Application of Geophyics to Engineering and Environmental Problems*. SAGEEP. https://doi.org/10.4133/sageep.29-057.

Junner, N. R. (1941). The Accra earthquake of June 22, 1939. *Gold Coast Geological Survey Bulletin*, 13:1–47.

Kadiri, U. A. and Amponsah, P. E. (2021). Computation of area-characteristic seismicity parameters in Ghana, Nigeria, and immediate neighbors. *Arabian Journal of Geosciences*, 14(13):1264. https://doi.org/10.1007/s12517-021-07558-6.

Kwayisi, D., Nyavor, E., Dzikunoo, E. A., Fynn, I. E. M., Kutu, J., and Nude, P. M. (2023). Cryogenian-Ediacaran crustal growth and evolution of the active margin of the Dahomeyide belt, Ghana. *Geological Magazine*, 160(10):1914–1931. https://doi.org/10.1017/S0016756823000808.

Lermo, J. and Chavez-Garcia, J. F. (1993). Site effect evaluation using spectral ratios with only one station. *Bulletin of the Seismological Society of America*, 83(5):1574–1594.

Liu, L., Chen, Q. F., Wang, W., and Rohrbach, E. (2014). Ambient noise as the new source for urban engineering seismology and earthquake engineering: A case study from Beijing metropolitan area. *Earthquake Science*, 27(1):89–100. https://doi.org/10.1007/s11589-013-0052-x.

Marcellini, A. (2006). Guidelines for the Implementation of the H/V Spectral Ratio Technique on Ambient Vibrations. Technical Report Deliverable D23.12, SESAME European Project. http://sesame-fp5.obs.ujf-grenoble.fr.

Meghraoui, M., Amponsah, P., Ayadi, A., Ayele, A., Ateba, B., Bensuleman, A., et al. (2016). The Seismotectonic Map of Africa. *Episodes*, 39(1):1–10. https://doi.org/10.18814/epiiugs/2016/v39i1/89232.

Meghraoui, M., Amponsah, P., Bernard, P., and Ateba, B. (2019). Active transform faults in the Gulf of Guinea: insights from geophysical data and implications for seismic hazard assessment. *Canadian Journal of Earth Sciences*, 56(11):1398–1408. https://doi.org/10.1139/cjes-2018-0247.

Molnar, S., Cassidy, J. F., Monahan, P. A., Onur, T., Ventura, C., and Rosenberger, A. (2007). Earthquake Site Response Studies Using Microtremor Measurements in Southwestern British Columbia. In *Ninth Canadian Conference on Earthquake Engineering*, pages 410–419, Ottawa, Canada.

Moustafa, S. S. R., Abdalzaher, M. S., Naeem, M., and Fouda, M. M. (2022). Seismic Hazard and Site Suitability Evaluation Based on Multicriteria Decision Analysis. *IEEE Access*, 10:69511–69530. https://doi.org/10.1109/ACCESS.2022.3186937.

Mundepi, A. K., Galiana-Merino, J. J., Asthana, A. K. L., and Rosa-Cintas, S. (2015). Soil characteristics in Doon Valley (north west Himalaya, India) by inversion of H/V spectral ratios from ambient noise measurements. *Soil Dynamics and Earthquake Engineering*, 77:309–320. https://doi.org/10.1016/j.soildyn.2015.06.006.

Murbach, D., Rockwell, T. K., and Bray, J. D. (1999). The Relationship of Foundation Deformation to Surface and Near-Surface Faulting Resulting from the 1992 Landers Earthquake. *Earthquake Spectra*, 15(1):121–144. https://doi.org/10.1193/1.1586032.

Nakamura, Y. (1997). Seismic vulnerability indices for ground and structures using microtremor. *World Congress on Railway Research*, pages 1–7.

Nakamura, Y., Sato, T., and Nishinaga, M. (2000). Local Site Effect of Kobe Based on Microtremor. In *Proceedings of the Sixth International Conference on Seismic Zonation*, pages 3–8, Palm Springs, California.

Nortey, G., Armah, T. K., and Amponsah, P. (2018). Vs30 mapping at selected sites within the Greater Accra Metropolitan Area. *Journal of African Earth Sciences*, 142:158–169. https://doi.org/10.1016/j.jafrearsci.2018.02.020.

Oettle, N. K. and Bray, J. D. (2013). Geotechnical Mitigation Strategies for Earthquake Surface Fault Rupture. *Journal of Geotechnical and Geoenvironmental Engineering*, 139(11):1864–1874. https://doi.org/10.1061/(asce)gt.1943-5606.0000933.

Onyebueke, E., Durrheim, R., and Manzi, M. (2017). Assessment of Site Effect at the Seismological Stations in South Africa Using the HVSR Technique. In *11th SAGA Biennial Technical Meeting and Exhibition*, Swaziland.

Owusu, G. (2012). Coping with Urban Sprawl: A Critical Discussion of the Urban Containment Strategy in a Developing Country City, Accra. *The Journal of Urbanism*, 2:17.

Parolai, S. (2012). *Investigation of Site Responses in Urban Areas by Using Earthquake Data and Seismic Noise*, pages 1–41. GFZ. https://doi.org/10.2312/GFZ.NMSOP-2.

Ranjan, R. (2005). Seismic Response Analysis of Dehradun. Master's thesis, International Institute for Geo-Information Science and Earth Observations, Enschede, Netherlands.

SESAME (Site EffectS Assessment using AMbient Excitations) (2004). Guidelines for the implementation of the H/V spectral ratio technique on ambient vibrations measurements, processing and interpretation. Technical Report Deliverable D23.12, SESAME European Project.

Talha Qadri, S. M., Nawaz, B., Sajjad, S. H., and Sheikh, R. A. (2015). Ambient noise H/V spectral ratio in site effects estimation in Fateh jang area, Pakistan. *Earthquake Science*, 28(1):87–95. https://doi.org/10.1007/s11589-014-0105-9.

Tanjung, N. A. F., Permatasari, I., and Yuniarto, A. H. P. (2021). Mapping of weathered layer thickness and Seismic Vulnerability in Tegal using HVSR method. *Journal of Physics: Conference Series*, 1951(1):012053. https://doi.org/10.1088/1742-6596/1951/1/012053.

Tian, B., Du, Y., You, Z., and Zhang, R. (2019). Measuring the sediment thickness in urban areas using revised H/V spectral ratio method. *Engineering Geology*, 260:105223. https://doi.org/10.1016/j.enggeo.2019.105223.

Ullah, I. and Prado, R. L. (2017). Soft sediment thickness and shear-wave velocity estimation from the H/V technique up to the bedrock at meteorite impact crater site, Sao Paulo city, Brazil. *Soil Dynamics and Earthquake Engineering*, 94:215–222. https://doi.org/10.1016/j.soildyn.2017.01.015.

Vella, A., Galea, P., and D'Amico, S. (2013). Site frequency response characterisation of the Maltese islands based on ambient noise H/V ratios. *Engineering Geology*, 163:89–100. https://doi.org/10.1016/j.enggeo.2013.06.006.

Wathelet, M., Chatelain, J. L., Cornou, C., Giulio, G. D., Guillier, B., Ohrnberger, M., and Savvaidis, A. (2020). Geopsy: A user-friendly open-source tool set for ambient vibration processing. *Seismological Research Letters*, 91(3):1878–1889. https://doi.org/10.1785/0220190360.